

Multistage-batch bipolar membrane electrodialysis for base production from high-salinity wastewater

Arif Hussain, Haiyang Yan, Noor Ul Afsar, Chenxiao Jiang, Yaoming Wang (✉), Tongwen Xu (✉)

Department of Applied Chemistry, Anhui Provincial Engineering Laboratory of Functional Membrane Science and Technology,
School of Chemistry and Materials Science, University of Science and Technology of China, Hefei 230026, China

© Higher Education Press 2021

Abstract Bipolar membrane electrodialysis (BMED) is considered a state-of-the-art technology for the conversion of salts into acids and bases. However, the low concentration of base generated from a traditional BMED process may limit the viability of this technology for a large-scale application. Herein, we report an especially designed multistage-batch (two/three-stage-batch) BMED process to increase the base concentration by adjusting different volume ratios in the acid (V_{acid}), base (V_{base}), and salt compartments (V_{salt}). The findings indicated that performance of the two-stage-batch with a volume ratio of $V_{\text{acid}}:V_{\text{base}}:V_{\text{salt}} = 1:1:5$ was superior in comparison to the three-stage-batch with a volume ratio of $V_{\text{acid}}:V_{\text{base}}:V_{\text{salt}} = 1:1:2$. Besides, the base concentration could be further increased by exchanging the acid produced in the acid compartment with fresh water in the second stage-batch process. With the two-stage-batch BMED, the maximum concentration of the base can be obtained up to $3.40 \text{ mol} \cdot \text{L}^{-1}$, which was higher than the most reported base production by BMED. The low energy consumption and high current efficiency further authenticate that the designed process is reliable, cost-effective, and more productive to convert saline water into valuable industrial commodities.

Keywords bipolar membrane electrodialysis, multistage-batch, base production, high-salinity wastewater

1 Introduction

To date, large volumes of saline wastewater is discharging from various industries such as coal mining industry, power generation, pulp and paper, petrochemical industry and etc. For instance, according to the China Water

Resources Bulletin 2018, about 75 billion tons of wastewater is discharging every year in China, while the industrial saline wastewater accounts for one fourth of total volumes of wastewater. In addition, industrial saline wastewater has high salt content that causes destruction to the ecosystems, salinity of soils, and death of aquatic species. Therefore, industrial saline wastewater should be treated before released to the main stream [1]. In past decades, various methods for treating saline wastewater are biological treatment (salt-tolerant organisms) [2], absorption [3], ion exchanger [4], and hybrid membrane technologies ultrafiltration and reverse osmosis) [5]. Among these methods, membrane based technology is becoming a promising treatment that can dramatically reduce or completely eliminate the formation of secondary waste. Recently, novel technologies toward zero liquid discharge (ZLD) [6,7] are emerging which can meet with the strict legislation of wastewater disposal. The implementation of ZLD systems requires further concentration of brine, evaporation, and crystallization process to obtain dry salt. For instance, high-pressure reverse osmosis, membrane distillation [8], forward osmosis, and electrodialysis [9,10] have been applied for the concentration of brine to a very high salt content [2]. Nanofiltration is widely applied for the separation of monovalent/divalent salts and the reduction of waste discharge [7,11–15]. Multi-effect distillation, mechanical vapor compression are the most economically viable technologies for the concentration of salt [16,17]. Recently, bioinspired membrane based separation process has also been developed for high-efficient water treatment [18–20]. ZLD is a sustainable method from the viewpoint of circular economy [6]. But a major challenge for the implementing of ZLD is how to recycle the recovered salts. The recovered salts from a ZLD plant are usually considered as hazardous waste because these salts contain a small fraction of organic matters. The conventional procedures for the purification and production of the high-purity NaCl from natural brines

is the solar evaporation procedure where the multivalent salts (magnesium chloride, magnesium sulfate, and magnesium bromide) are settled out from the concentrated brine during the movement of brine from one pond to another. But for the recovered salts, the crystallization method is ineffective to separate salts from the organic matters. Moreover, the low added-value of the recovered salt also hinder the potential valorization of salts. As a result, the salt waste from the ZLD process is becoming a new kind of secondary pollutant that it is urgent to be treated.

Bipolar membrane electrodialysis (BMED) is a very promising process for the valorization of salt waste [21]. By taking the advantages of the accelerated water splitting in the BMED, this technology allows the concurrent conversion of the salt (such as NaCl) into the corresponding acid (HCl) and base (NaOH). Many industries use acid-base in their processes which also lead to the formation of saline wastewater such as NaCl, if the generated salt is split again into acid-base successfully, it may develop a circular economy with the maximum recovery of valuable components [5,22]. However, the concentrations of acid and base produced by a typical BMED are not very high (max base conc. $3.6 \text{ mol} \cdot \text{L}^{-1}$) which restrict the adaptability of the BMED technology. Referring to the recently published data about BMED, Ghyselbrecht et al. [23] performed a BMED experiment using saline water (NaCl and KCl), and reported a concentration of base $2 \text{ mol} \cdot \text{L}^{-1}$ with a high purity. Similarly, Reig et al. [24] reported the BMED generation of HCl and NaOH concentration up to 1.99 and $2.14 \text{ mol} \cdot \text{L}^{-1}$, respectively. Ibáñez et al. [25] used the BMED with softened reverse osmosis brine as feed in a bench-scale setup. The produced HCl and NaOH concentrations were around 0.8 and $1.0 \text{ mol} \cdot \text{L}^{-1}$, respectively [25]. Xue et al. [26] treated the sodium acetate residue using a BMED technology and a $0.556 \text{ mol} \cdot \text{L}^{-1}$ of NaOH was reported. Recently, Herrero-Gonzalez et al. [27] reported the BMED production of HCl and NaOH up to ca. 3.3 and ca. $3.6 \text{ mol} \cdot \text{L}^{-1}$, respectively. They concluded that concentrations were almost 50% higher than any other reported in the literature. The specific energy consumptions were in the range of $21.8\text{--}43.5 \text{ kWh} \cdot \text{kg}^{-1}$ of HCl. But the specific energy consumption for base generation was not considered. In the market, the price of base (NaOH) is much higher than the price of acid such as HCl in the practical case. To increase the concentration of base and decrease the energy consumption for base generation is the foremost thing for the BMED process.

The main reason that restricts the concentration of base or acid in BMED process is the transport of water molecules through the ion exchange membrane via electro-osmosis and concentration-gradient osmosis. The electro-osmosis is caused by the electro-migration of hydrated ions from salt compartment to the acid or base compartment diluting the acid or base concentration. This factor is more pronounced for the generation of higher

concentration of base and acid. In the latter period of BEMD experiments, the osmotic-pressure difference between the acid/base compartment and salt compartment will accelerate the transport of water molecules from the salt compartment into the acid or base compartment [7]. Previous studies on BMED were mainly focused on the optimization of operating parameters such as current density, voltage drop, temperature, and flow velocity. These experiments were performed on batch or single-stage BMED for the conversion of salt into acid and base, in which the concentration gradient is relatively high. Unfortunately, the multi-stage cascade, a widely adopted strategy in the electrodialysis [28,29], has been rarely reported in the BMED process.

In this research, the main objective is to investigate the feasibility of multistage-batch BMED experiment including two-stage-batch and three-stage-batch for highly concentrated base generation. We studied the effect of change in salt compartment solution or both acid and salt compartment in multi stage batch (two/three stage) for volume ratio $V_{\text{acid}}:V_{\text{base}}:V_{\text{salt}} = 1:1:5$ and $V_{\text{acid}}:V_{\text{base}}:V_{\text{salt}} = 1:1:2$, aiming to obtain high base concentration. The optimized current density of $50 \text{ mA} \cdot \text{cm}^{-2}$ was applied during the experimental process. Results indicate that two stage with a volume ratio of $V_{\text{acid}}:V_{\text{base}}:V_{\text{salt}} = 1:1:5$ with changing both acid and salt compartment solution show high concentration of base ($3.4 \text{ mol} \cdot \text{L}^{-1}$) with a low energy consumption of ($1.54\text{--}1.9 \text{ kW} \cdot \text{h}^{-1}$) in first and second stages.

2 Experimental

2.1 Materials

The ion exchange membranes and bipolar membranes used for BMED were CM-2 (a cation exchange membrane (CEM)), AM-1 (an anion exchange membrane (AEM)) and BP-1E (a bipolar membrane), which were all purchased from ASTOM Corp, Japan; the physiochemical properties are illustrated in Table 1. All the chemicals are AR grade and purchased from Sinopharm Chemical Reagent. Deionized water was used.

2.2 BMED apparatus

The BMED setup, principle and digital photograph is shown in Fig. 1. Figure 1(a) shows the BMED setup that consists of different units such as power supply, membrane stack, pumps and different compartments. Figure 1(b) shows the BMED stack in detail, which consists of a set of membranes, i.e., five CM-2, four BP-1E, and four AM-1 membranes, forming four acid compartments, four base compartments, and four feed compartments, respectively. The membrane with an effective area 189 cm^2 was separated using a spacer (0.75 mm) in the BMED stack.

Table 1 The main properties of the membranes used for the experiments ^{a)}

Membrane	Thickness /mm	Tensile strength /MPa	Area resistance /($\Omega \cdot \text{cm}^2$)	Functional group	Reinforcing membrane matrix	Burst strength /MPa	Water splitting voltage/V	Water splitting efficiency
AM-1	0.11–0.16	≥ 0.20	1.2–2.0	$\text{R}_4\text{-N}^+$	PS-DVB + PVC	—	—	—
CM-2	0.11–0.16	≥ 0.15	2.0–4.5	R-SO_3^-	PS-DVB + PVC	—	—	—
BP-1E	0.22	—	—	—	—	≥ 0.40	1.2	> 0.98

a) The data was obtained from the manufacturer. PS, polystyrene; DVB, divinylbenzene; PVC, polyvinyl chloride.

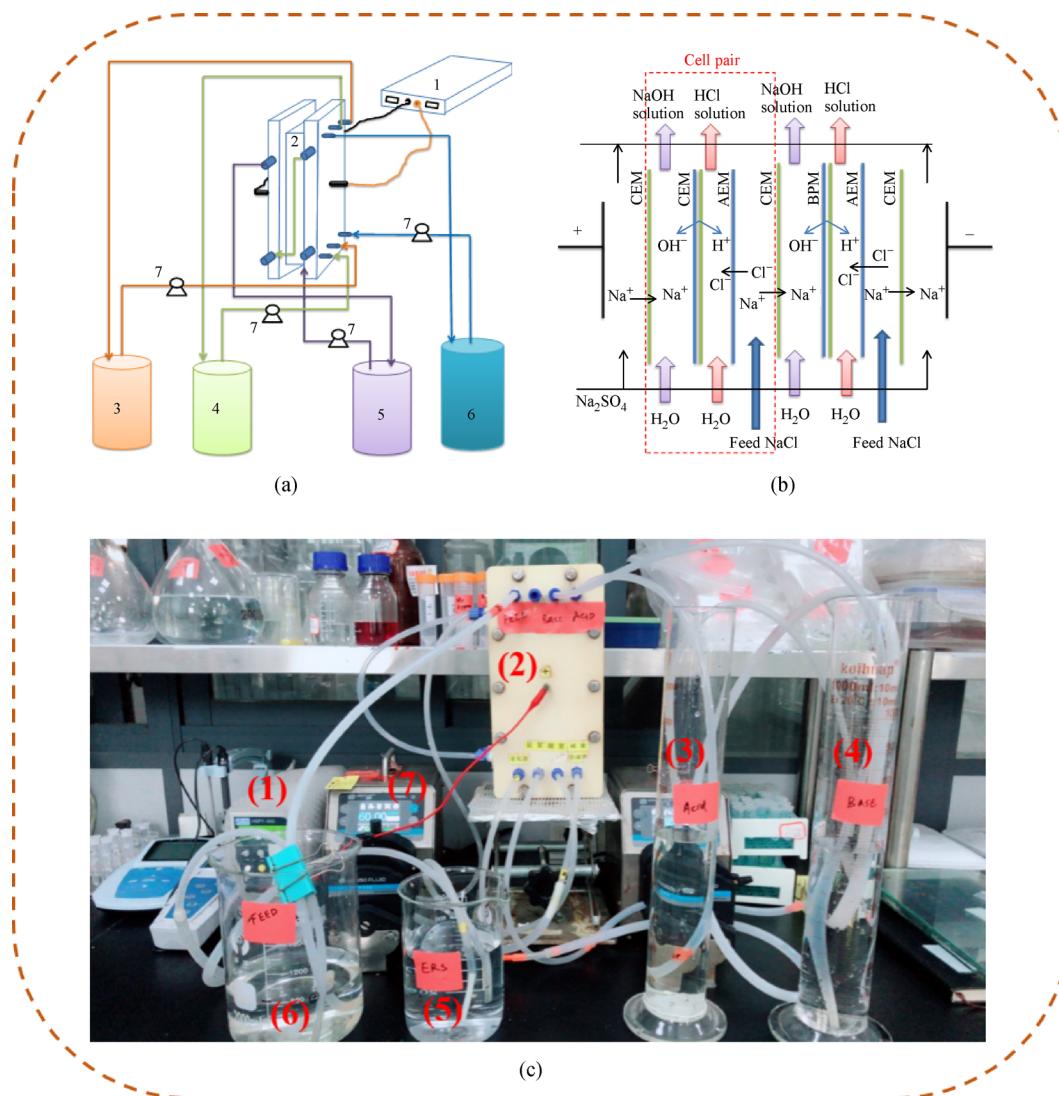


Fig. 1 (a) Schematic BMED setup containing (1) a direct current power supply, (2) a membrane stack with four cell pairs, (3) acid chamber, (4) base chamber, (5) rinse solution, (6) feed chamber, and (7) peristaltic pumps; (b) schematic diagram of the BMED cell configuration assemble with CEM, bipolar membrane and AEM; (c) the digital photo of BMED system.

Three different solutions were used in experiment, (a) feed solution (NaCl , 3.5 wt-%), (b) electrode rinse solution (Na_2SO_4 , $0.3 \text{ mol} \cdot \text{L}^{-1}$, 500 mL), and (c) deionized water (400 mL) as initial solution for acid and base compartments. The flow rates of various streams were controlled by the peristaltic pumps (BT600L with $2 \times \text{YT15}$ pump head, Baoding Lead Fluid Technology Co. Ltd., China) at

flow rate of $400 \text{ mL} \cdot \text{min}^{-1}$. The digital photo of BMED system is shown in Fig. 1(c).

2.3 Experimental design

A high concentration of base solution was produced through multistage-batch BMED process as shown in

Fig. 2. Four operation modes were designed and investigated, including (a) three-stage-batch BMED with changing salt solution, (b) two-stage-batch BMED with changing salt solution, and (c) two-stage-batch BMED with changing salt and acid solutions. The volume ratio between acid, base and salt solutions ($V_{\text{acid}}:V_{\text{base}}:V_{\text{salt}}$) was set as 1:1:2 in mode (a), while that was set as 1:1:5 in modes (b) and (c). In the multistage-batch BMED process, each batch was operated at constant-current mode at a current density of $50 \text{ mA} \cdot \text{cm}^{-2}$ (9.45 A). During each batch operation, the conductivity of the feed compartment was monitored by a conductivity meter (DDS-307, Shanghai INESA & Scientific Instrument Co., Ltd., China). The experiment was stopped once the conductivity

of the feed solution decreased to $10 \text{ mS} \cdot \text{cm}^{-1}$. Samples were taken in different interval of time from acid and base compartment to measure the concentration of NaOH and HCl by titration.

2.4 Data calculation and evaluation

Current efficiency (η , %) and energy consumption (E , $\text{kWh} \cdot \text{kg}^{-1}$) are the important parameters to evaluate the performance of BMED process and were calculated from the concentration of acid and base produced during the BMED process. Volume change was also considered during calculating current efficiency and energy consumption. The current efficiency η is given by Eq. (1):

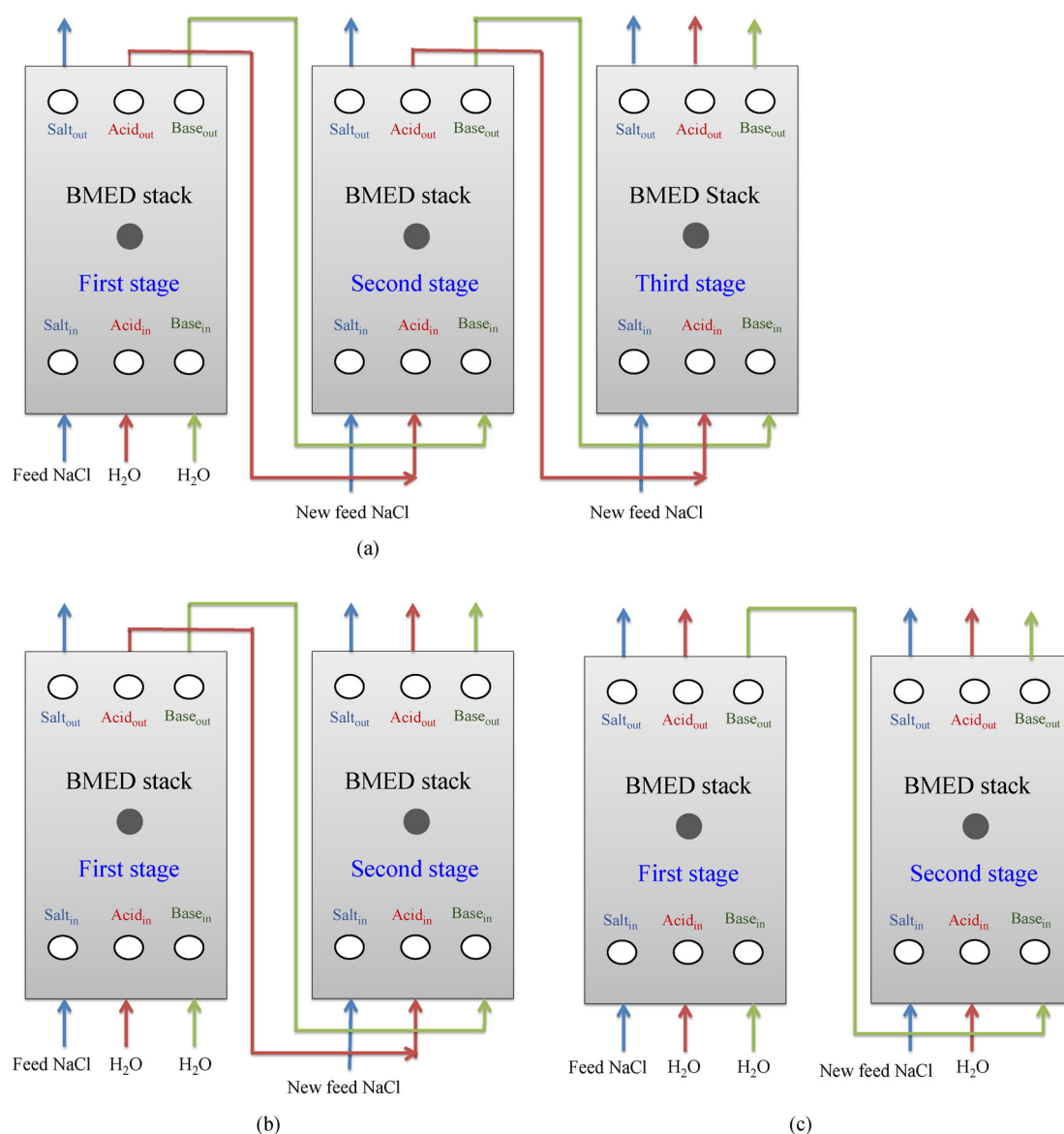


Fig. 2 Schemes for multistage-batch BMED design: (a) three-stage-batch BMED with changing salt solution ($V_{\text{acid}}:V_{\text{base}}:V_{\text{salt}} = 1:1:2$); (b) two-stage-batch BMED with changing salt solution ($V_{\text{acid}}:V_{\text{base}}:V_{\text{salt}} = 1:1:5$); (c) two-stage-batch BMED with changing salt and acid solutions ($V_{\text{acid}}:V_{\text{base}}:V_{\text{salt}} = 1:1:5$).

$$\eta = \frac{(C_t V_t - C_0 V_0) F}{\int N I dt} \times 100\%, \quad (1)$$

where C_t and C_0 are the concentrations of acid or base solution at time t and 0 respectively, V_t and V_0 are the volumes of acid or base solutions at time t and 0 respectively, F is the faraday constant ($96485 \text{ C} \cdot \text{mol}^{-1}$), and I is the current applied during the BMED process ($I = 9.45 \text{ A}$).

The energy consumption ($\text{kWh} \cdot \text{kg}^{-1}$) is calculated according to Eq. (2):

$$E = \int \frac{U_{\text{cell pairs}} I dt}{(C_t V_t - C_0 V_0) M} = \int \frac{(U_{\text{stack}} - U_{\text{electrode compartments}}) I dt}{(C_t V_t - C_0 V_0) M}, \quad (2)$$

where $U_{\text{cell pairs}}$ is the voltage drop across the four cell pairs, U_{stack} is the voltage drop across the membrane stack, $U_{\text{electrode compartments}}$ is the total voltage drop of cathode and anode compartments, which can be calculated

by the previous method [28], and M is the molar weight of acid or base.

3 Results and discussion

3.1 Three-stage-batch BMED with changing salt solution

Three-stage-batch BMED was carried to produce high concentration of base solution. Here, the desalinated feed solution was discharged after each stage, and a new feed solution was feed in the salt compartment in next stage. In the three-stage-batch BMED process, the volume ratio between acid, base and salt solutions ($V_{\text{acid}}:V_{\text{base}}:V_{\text{salt}}$) was set as 1:1:2. A constant-current density of $50 \text{ mA} \cdot \text{cm}^{-2}$ was applied for BMED stack.

Figure 3 shows the BMED performances as a function of time. In each stage, the conductivity of salt solution can be decreased to $10 \text{ mS} \cdot \text{cm}^{-1}$ as shown in Fig. 3(a). However, the conductivity of salt solution increases first, and then decreases as a function of time. The reason can be ascribed to the acid leakage from the acid compartment to the salt

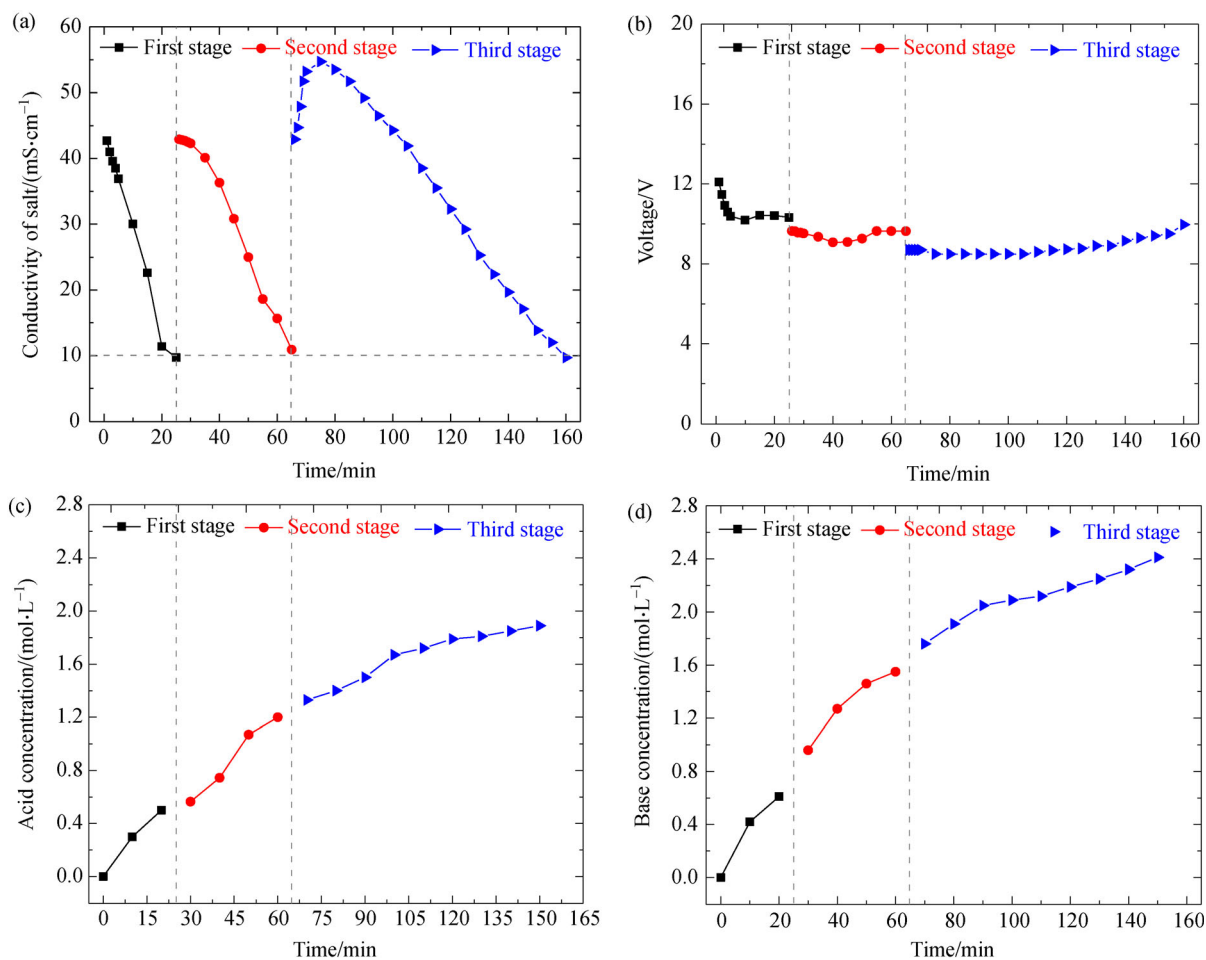


Fig. 3 BMED performance in three-stage-batch BMED with changing salt solution: (a) conductivity of salt solution, (b) membrane stack voltage, (c) acid concentration, and (d) base concentration (note: $V_{\text{acid}}:V_{\text{base}}:V_{\text{salt}} = 1:1:2$).

compartment [30–32]. As the stage advances, the voltage across the membrane stack exhibits a decreasing trend since that the concentration of the produced acid and base increases gradually as can be seen in Figs. 3(c) and 3(d). After three-stage-batch BMED, the acid concentration can reach to 0.5, 1.2, and 1.89 mol·L⁻¹ in first, second, and third stages, respectively; while the base concentration can reach to 0.69, 1.55, and 2.41 mol·L⁻¹, respectively.

Besides, the energy consumption and current efficiency were calculated as shown in Table 2. It can be seen that the energy consumption in first stage is similar to that in second stage. However, the energy consumption in third stage is higher than that in the first two stages. The reason is that the running time of the third stage is longer, resulting in an increase in $\int U_{\text{cell pairs}} Idt$. As a consequence, the energy consumption increases as the stage advances. The current efficiency decreases as the stage advances, which is caused by the longer running time according to the Eq. (1). For instance, the current efficiency for NaOH decreases from 66.05% to 38.79% rapidly as the stage advances.

3.2 Two-stage-batch BMED with changing salt solution

As mentioned above, three-stage-batch BMED was carried to produce high concentration of base solution. However, the concentration of the produced base is not high enough. Previous report has indicated that high volume ratio of dilute to concentrate in electrodialysis process can produce highly concentrated solution [28,31]. Therefore, the volume ratio between acid, base and salt solutions ($V_{\text{acid}}:V_{\text{base}}:V_{\text{salt}}$) was changed to 1:1:5 compared with the above section. In addition, two-stage-batch BMED was designed. Specifically, the desalinated feed solution was discharged after the first stage, and a new feed solution was feed in the salt compartment in the second stage. A constant-current density of 50 mA·cm⁻² was applied for BMED stack.

Figure 4 shows the two-stage-batch BMED performance. In both stages, the conductivity of salt solution was decreased to 10 mS·cm⁻¹ as shown in Fig. 4(a). The running time of the second stage (100 min) is longer than that of the first stage (80 min). The voltage across the membrane stack was stable at the range of 8–12 V. In the first stage, the acid and base concentrations can reach to 1.09 and 2.30 mol·L⁻¹, respectively. Both values are higher than that in the three-stage-batch BMED process; the reason is that the $V_{\text{acid}}:V_{\text{base}}:V_{\text{salt}}$ was changed as 1:1:5 in two-stage-batch BMED. Herein, the acid concentration

is much lower than the base concentration, which can be ascribed to the acid leakage from the acid compartment to the salt compartment due to the lower proton blocking performance of the used AM-1. Compared with OH⁻ ions, the protons have smaller in size and higher in ion mobility. The leakage of H⁺ across the anion-exchange membrane is more pronounced compared with the leakage of OH⁻ ions across the cation-exchange membrane. This phenomenon was consistent with numerous studies that the acid concentration is lower than the alkali concentration for the BMED process [33–36]. In the second stage, the concentration of acid and base can be increased to 2.30 and 2.91 mol·L⁻¹, respectively. Both values are higher than that in the third stage as mentioned above. Besides, the energy consumption and current efficiency for NaOH increases and decreases as the stage advances respectively as shown in Table 3. The reason can be ascribed to the longer running time with relatively less amount of produced NaOH according to Eqs. (1) and (2). While for HCl, on the contrary, the energy consumption and current efficiency decreases and increases as the stage advances, respectively. The reason may be that the acid leakage in the second stage is lower than that in the first stage, because the produced acid in the second stage is larger than that in the first stage as shown in Fig. 4(c).

In overall, the BMED performance of two-stage-batch ($V_{\text{acid}}:V_{\text{base}}:V_{\text{salt}} = 1:1:5$) is better than that of three-stage-batch ($V_{\text{acid}}:V_{\text{base}}:V_{\text{salt}} = 1:1:2$) in consideration of the high concentration of the produced acid and base.

3.3 Two-stage-batch BMED with changing salt and acid solutions

In multistage BMED process, it is hard to avoid acid leakage because of the poor proton blocking performance of AEMs [30]. However, the acid leakage should be controlled to produce much higher base concentration to meet the requirement of industrial application. Generally, the acid leakage is caused by two driving forces including concentration diffusion and electro-migration [31]. In BMED process, the concentration gradient of H⁺ ions between the acid and salt compartment increases as a function of time. Under a constant current operation mode, the acid leakage caused by the electro-migration should remain unchanged. However, the acid leakage caused by the concentration diffusion would exhibit an increasing trend due to the increased concentration gradient of H⁺ ions between the acid and salt compartment, which is

Table 2 Energy consumption and current efficiency in three-stage-batch BMED with changing salt solution

$V_{\text{acid}}:V_{\text{base}}:V_{\text{salt}}$	Stage	Energy consumption/(kWh·kg ⁻¹)		Current efficiency/%	
		HCl	NaOH	HCl	NaOH
1:1:2	First	2.13	1.44	48.92	66.05
	Second	1.95	1.45	45.73	56.00
	Third	3.56	2.62	31.24	38.79

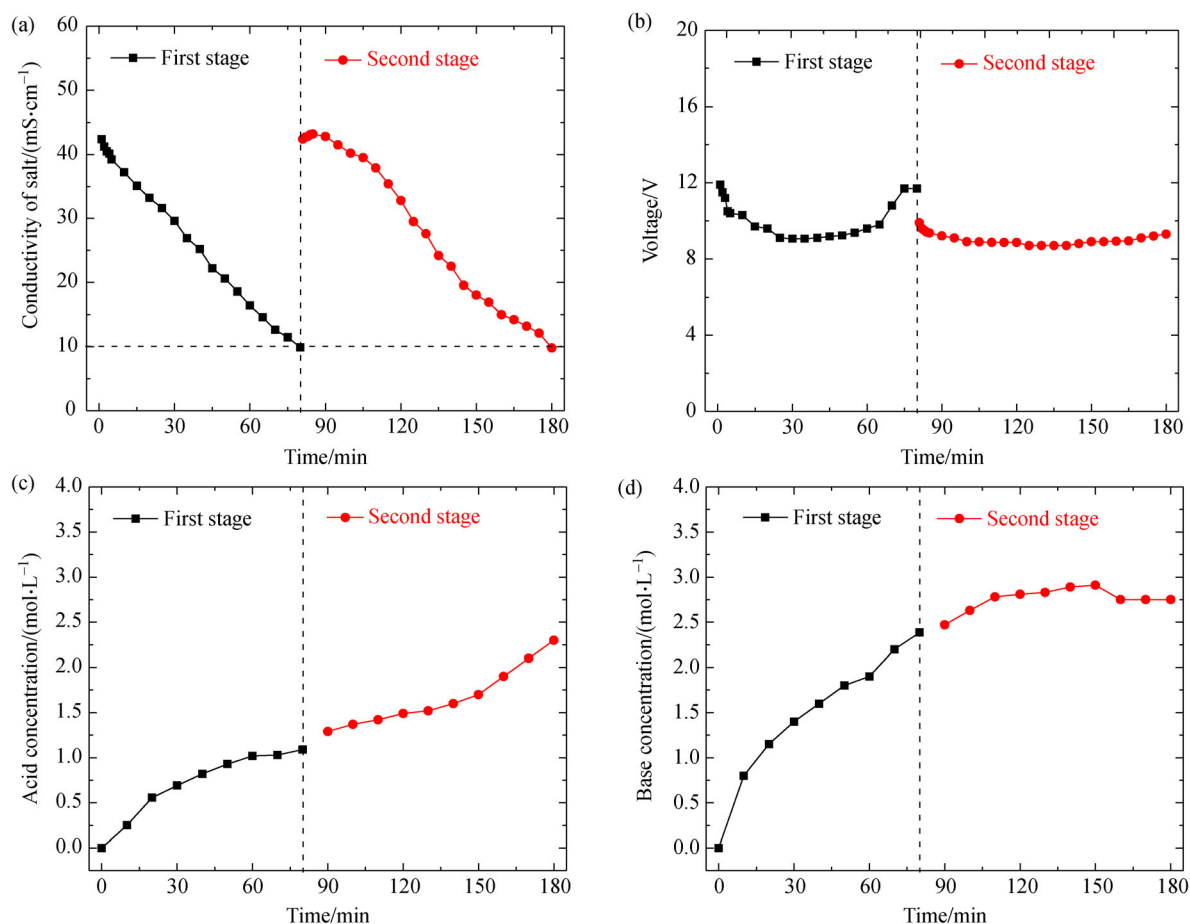


Fig. 4 BMED performance in two-stage-batch BMED with changing salt solution: (a) conductivity of salt solution, (b) membrane stack voltage, (c) acid concentration, and (d) base concentration (note: $V_{\text{acid}}:V_{\text{base}}:V_{\text{salt}} = 1:1:5$).

Table 3 Energy consumption and current efficiency in two-stage-batch BMED with changing salt solution

$V_{\text{acid}}:V_{\text{base}}:V_{\text{salt}}$	Stage	Energy consumption ($\text{kWh}\cdot\text{kg}^{-1}$)		Current efficiency/%	
		HCl	NaOH	HCl	NaOH
1:1:5	First	3.44	1.52	28.98	59.93
	Second	2.43	2.65	34.54	28.81

disadvantageous for the base production with a much high concentration. Hence, in two-stage-batch BMED, the operation mode was changed as follows. The desalinated feed solution and produced acid solution were both discharged after the first stage, and a new feed solution and fresh water were feed in the salt compartment and acid compartment respectively in the second stage.

Figure 5 shows the BMED performance as a function of time. We can see that in the second stage, the acid concentration increases from 0 to $1.57\text{ mol}\cdot\text{L}^{-1}$, while the base concentration increases from 2.30 to as high as $3.40\text{ mol}\cdot\text{L}^{-1}$. In this process, the acid concentration was lower than that in the above section. Therefore, the concentration of H^+ ions between the acid and salt compartment was low, and then low acid leakage. Accordingly, the base

concentration can be increased much more compared with the above section as shown in Fig. 5(d). Meanwhile, the energy consumption for NaOH in the second stage can also be decreased to $1.90\text{ kWh}\cdot\text{kg}^{-1}$ (Table 4), lower than that in the above section ($2.65\text{ kWh}\cdot\text{kg}^{-1}$). Besides, the current efficiency for NaOH in the second stage can be increased to 41.73% (Table 4), higher than that in the above section (28.81%).

In overall, in two-stage-batch BMED, the high concentration base solution can be produced when both the desalinated feed solution and produced acid solution were discharged after the first stage, and a new feed solution and fresh water were feed in the salt compartment and acid compartment respectively in the second stage. Besides, the operating energy consumption is relatively low.

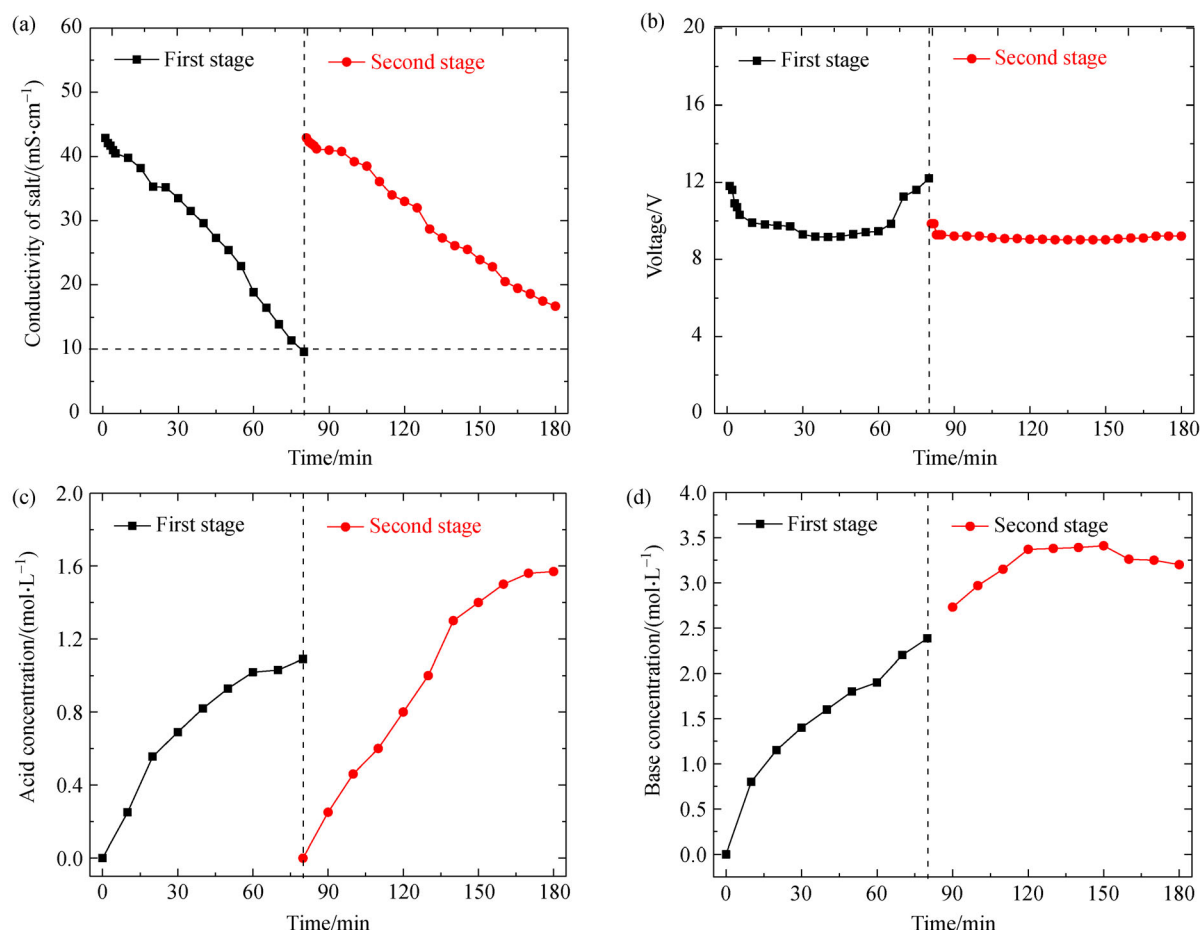


Fig. 5 BMED performance in two-stage-batch BMED with changing salt and acid solutions: (a) conductivity of salt solution, (b) membrane stack voltage, (c) acid concentration, and (d) base concentration (note: $V_{\text{acid}}:V_{\text{base}}:V_{\text{salt}}$ is 1:1:5).

Table 4 Energy consumption and current efficiency in two-stage-batch BMED with changing salt and acid solutions

$V_{\text{acid}}:V_{\text{base}}:V_{\text{salt}}$	Stage	Energy consumption/($\text{kWh}\cdot\text{kg}^{-1}$)		Current efficiency/%	
		HCl	NaOH	HCl	NaOH
1:1:5	First	3.49	1.54	28.98	59.93
	Second	2.36	1.90	36.73	41.73

3.4 Multistage-batch BMED performance evaluation

In the BMED process, high concentration of the acid and base solution is usually expected. Researchers have focused only on single stage BMED for acid and base production [24,37–41], in which acid and base can be concentrated to as high as 2.0 for acid and 2.5 $\text{mol}\cdot\text{L}^{-1}$ for base. How to further improve the concentration of the produced acid and base solutions? Multistage-batch BMED maybe an advanced method for producing highly concentrated acid and base solutions. Table 5 shows the production of maximum NaOH via BMED technology using different feed concentration compared with this work. The initial feed concentration in this work

(0.5 $\text{mol}\cdot\text{L}^{-1}$ NaCl) was equal to the seawater salinity (NaCl 3.5 wt-%), lower than the feed concentration of some reported researches [24,27,37,38,40,41]. Although, the maximum concentrations of the produced acid (2.30 $\text{mol}\cdot\text{L}^{-1}$) and base (3.40 $\text{mol}\cdot\text{L}^{-1}$) in this study are higher than the reported values. This should be ascribed to the advantageous of multistage-batch BMED as aforementioned.

4 Conclusions

In this study, multistage-batch BMED was proposed to convert salt to highly concentrated acid and base solutions.

Table 5 Summary of HCl and NaOH production using different concentration of NaCl as feed in BMED process

NaCl feed Concentration /($\text{mol} \cdot \text{L}^{-1}$)	Mode of operation	Max. HCl Concentration /($\text{mol} \cdot \text{L}^{-1}$)	Max. NaOH Concentration /($\text{mol} \cdot \text{L}^{-1}$)	Current efficiency /%	Energy consumption /($\text{kWh} \cdot \text{kg}^{-1}$)	Ref.
0.5	Multistage-batch	2.30	3.40	59–41	1.54–1.9	This work
1.71, 3.42	Batch	1.99	2.14	55–88	1.7	[24]
ca. 1.00	Semi continuous	0.98	1.64	44	7.3–4.4	[27]
0.02	Batch	ca. 0.2	ca. 0.2	85–35	–	[39]
0.6	Batch	0.22	0.29	95	–	[38]
0.048–0.390	Continuous	0.05–0.30	0.04–0.30	–	0.09	[42]
ca. 1.00	Batch	0.8	1	61–80	1.94–2.51	[37]
0.65	Batch	0.7	0.4	74–50	7.6–8.2	[40]
1.2	Batch	1.6	1.7	–	–	[41]

Three-stage-batch BMED and two-stage-batch BMED were designed with different $V_{\text{acid}}:V_{\text{base}}:V_{\text{salt}}$. Results indicate that BMED performance of two-stage-batch with $V_{\text{acid}}:V_{\text{base}}:V_{\text{salt}} = 1:1:5$ is superior to that of three-stage-batch with $V_{\text{acid}}:V_{\text{base}}:V_{\text{salt}} = 1:1:2$. Because the maximum concentrations of the produced acid and base in two-stage-batch BMED are the highest, and the energy consumption is relatively low. Additionally, in two-stage-batch BMED, the operation mode was investigated to further improve the concentration of the produced acid and base solutions. During the two-stage-batch BMED process, the base concentration can be improved further when the produced acid in the first stage was discharged and fresh water was used as initial solution feed into acid compartment in the second stage-batch. Hence, high concentration of base solution ($3.40 \text{ mol} \cdot \text{L}^{-1}$) can be produced by two-stage-batch BMED with $V_{\text{acid}}:V_{\text{base}}:V_{\text{salt}} = 1:1:5$. Further studies should be investigated for the optimization of membrane type, salt concentration, current density, and so on. Also, membrane fouling needs to be considered when treating the industrial waste salts.

Acknowledgements This project was supported by the National Natural Science Foundation of China (Grant Nos. 22061132003 and 22008226), the Key Technologies R & D Program of Anhui Province (Grant No. 202003a05020052), and the Major Science and Technology Innovation Projects in Shandong Province (Grant No. 2019JZZY010511).

References

- Lefebvre O, Moletta R. Treatment of organic pollution in industrial saline wastewater: a literature review. *Water Research*, 2006, 40(20): 3671–3682
- Tong T, Elimelech M. The global rise of zero liquid discharge for wastewater management: drivers, technologies, and future directions. *Environmental Science & Technology*, 2016, 50(13): 6846–6855
- Subramani A, Jacangelo J G. Treatment technologies for reverse osmosis concentrate volume minimization: a review. *Separation and Purification Technology*, 2014, 122: 472–489
- Oren Y, Korngold E, Daltrophe N, Messalem R, Volkman Y, Aronov L, Weismann M, Bouriakov N, Glueckstern P, Gilron J. Pilot studies on high recovery BWRO-EDR for zero liquid discharge approach. *Desalination*, 2010, 261(3): 321–330
- Herrero-Gonzalez M, Wolfson A, Dominguez-Ramos A, Ibañez R, Irabien A. Monetizing environmental footprints: index development and application to a solar-powered chemicals self-supplied desalination plant. *ACS Sustainable Chemistry & Engineering*, 2018, 6(11): 14533–14541
- Yao J, Wen D, Shen J, Wang J. Zero discharge process for dyeing wastewater treatment. *Journal of Water Process Engineering*, 2016, 11: 98–103
- Xiao H, Shao D, Wu Z, Peng W, Akram A, Wang Z, Zheng L, Xing W, Sun S. Zero liquid discharge hybrid membrane process for separation and recovery of ions with equivalent and similar molecular weights. *Desalination*, 2020, 482: 114387
- Marni Sandid A, Bassyouni M, Nehari D, Elhenawy Y. Experimental and simulation study of multichannel air gap membrane distillation process with two types of solar collectors. *Energy Conversion and Management*, 2021, 243: 114431
- Hulme A, Davey C, Tyrrel S, Pidou M, McAdam E. Transitioning from electrodialysis to reverse electrodialysis stack design for energy generation from high concentration salinity gradients. *Energy Conversion and Management*, 2021, 244: 114493
- Mir N, Bicer Y. Integration of electrodialysis with renewable energy sources for sustainable freshwater production: a review. *Journal of Environmental Management*, 2021, 289: 112496
- Xiao H, Chu C, Xu W, Chen B, Ju X, Xing W, Sun S. Amphibian-inspired amino acid ionic liquid functionalized nanofiltration membranes with high water permeability and ion selectivity for pigment wastewater treatment. *Journal of Membrane Science*, 2019, 586: 44–52
- Xu Y, Wang Z, Cheng X, Xiao Y, Shao L. Positively charged nanofiltration membranes via economically mussel-substance-simulated co-deposition for textile wastewater treatment. *Chemical Engineering Journal*, 2016, 303: 555–564
- Cao X, Zhou F, Cai J, Zhao Y, Liu M, Xu L, Sun S. High-

- permeability and anti-fouling nanofiltration membranes decorated by asymmetric organic phosphate. *Journal of Membrane Science*, 2021, 617: 118667
14. Cao X, Guo J, Cai J, Liu M, Japip S, Xing W, Sun S. The encouraging improvement of polyamide nanofiltration membrane by cucurbituril-based host-guest chemistry. *AIChE Journal*. American Institute of Chemical Engineers, 2020, 66(4): e16879
15. Lau W, Gray S, Matsuura T, Emadzadeh D, Chen J, Ismail A. A review on polyamide thin film nanocomposite (TFN) membranes: history, applications, challenges and approaches. *Water Research*, 2015, 80: 306–324
16. Liang L, Han D, Ma R, Peng T. Treatment of high-concentration wastewater using double-effect mechanical vapor recompression. *Desalination*, 2013, 314: 139–146
17. Alkhudhiri A, Darwish N, Hilal N. Membrane distillation: a comprehensive review. *Desalination*, 2012, 287: 2–18
18. Yang X, Yan L, Ran F, Huang Y, Pan D, Bai Y, Shao L. Mussel-/diatom-inspired silicified membrane for high-efficiency water remediation. *Journal of Membrane Science*, 2020, 597: 117753
19. Yang X, Yan L, Ma J, Bai Y, Shao L. Bioadhesion-inspired surface engineering constructing robust, hydrophilic membranes for highly-efficient wastewater remediation. *Journal of Membrane Science*, 2019, 591: 117353
20. Wang Z, Lau C, Zhang N, Bai Y, Shao L. Mussel-inspired tailoring of membrane wettability for harsh water treatment. *Journal of Materials Chemistry. A, Materials for Energy and Sustainability*, 2015, 3(6): 2650–2657
21. Xu T, Huang C. Electrodialysis-based separation technologies: a critical review. *AIChE Journal*. American Institute of Chemical Engineers, 2008, 54(12): 3147–3159
22. Herrero-Gonzalez M, Admon N, Dominguez-Ramos A, Ibañez R, Wolfson A, Irabien A. Environmental sustainability assessment of seawater reverse osmosis brine valorization by means of electrodialysis with bipolar membranes. *Environmental Science and Pollution Research International*, 2020, 27(2): 1256–1266
23. Ghyselbrecht K, Huygebaert M, Van der Bruggen B, Ballet R, Meesschaert B, Pinoy L. Desalination of an industrial saline water with conventional and bipolar membrane electrodialysis. *Desalination*, 2013, 318: 9–18
24. Reig M, Casas S, Valderrama C, Gibert O, Cortina J L. Integration of monopolar and bipolar electrodialysis for valorization of seawater reverse osmosis desalination brines: production of strong acid and base. *Desalination*, 2016, 398: 87–97
25. Ibáñez R, Pérez-González A, Gómez P, Urtiaga A M, Ortiz I. Acid and base recovery from softened reverse osmosis (RO) brines. Experimental assessment using model concentrates. *Desalination*, 2013, 309: 165–170
26. Xue S, Wu C, Wu Y, Chen J, Li Z. Bipolar membrane electrodialysis for treatment of sodium acetate waste residue. *Separation and Purification Technology*, 2015, 154: 193–203
27. Herrero-Gonzalez M, Diaz-Guridi P, Dominguez-Ramos A, Ibañez R, Irabien A. Photovoltaic solar electrodialysis with bipolar membranes. *Desalination*, 2018, 433: 155–163
28. Yan H, Wang Y, Wu L, Shehzad M, Jiang C, Fu R, Liu Z, Xu T. Multistage-batch electrodialysis to concentrate high-salinity solutions: process optimisation, water transport, and energy consumption. *Journal of Membrane Science*, 2019, 570–571: 245–257
29. Doornbusch G, Tedesco M, Post J, Borneman Z, Nijmeijer K. Experimental investigation of multistage electrodialysis for seawater desalination. *Desalination*, 2019, 464: 105–114
30. Koter S, Warszawski A. A new model for characterization of bipolar membrane electrodialysis of brine. *Desalination*, 2006, 198(1–3): 111–123
31. Yan H, Wu L, Wang Y, Irfan M, Jiang C, Xu T. Ammonia capture from wastewater with a high ammonia nitrogen concentration by water splitting and hollow fiber extraction. *Chemical Engineering Science*, 2020, 227: 115934
32. Takagi R, Vasselbehagh M, Matsuyama H. Theoretical study of the permselectivity of an anion exchange membrane in electrodialysis. *Journal of Membrane Science*, 2014, 470(9): 486–493
33. Lorrain Y, Pourcelly G, Gavach C. Transport mechanism of sulfuric acid through an anion exchange membrane. *Desalination*, 1997, 109(3): 231–239
34. Miyoshi H. Diffusion coefficients of ions through ion-exchange membranes for Donnan dialysis using ions of the same valence. *Chemical Engineering Science*, 1997, 52(7): 1087–1096
35. Palaty Z, Zakova A. Transport of some strong incompletely dissociated acids through anion-exchange membrane. *Journal of Colloid and Interface Science*, 2003, 268(1): 188–199
36. Beck A, Ernst M. Kinetic modeling and selectivity of anion exchange in Donnan dialysis. *Journal of Membrane Science*, 2015, 479: 132–140
37. Thiel G, Kumar A, Gómez-González A, Lienhard J. Utilization of desalination brine for sodium hydroxide production: technologies, engineering principles, recovery limits, and future directions. *ACS Sustainable Chemistry & Engineering*, 2017, 5(12): 11147–11162
38. Lin H, Cejudo-Marín R, Jeremiasse A W, Rabaey K, Yuan Z, Pikaar I. Direct anodic hydrochloric acid and cathodic caustic production during water electrolysis. *Scientific Reports*, 2016, 6(1): 20494
39. Badruzzaman M, Oppenheimer J, Adham S, Kumar M. Innovative beneficial reuse of reverse osmosis concentrate using bipolar membrane electrodialysis and electrochlorination processes. *Journal of Membrane Science*, 2009, 326(2): 392–399
40. Yang Y, Gao X, Fan A, Fu L, Gao C. An innovative beneficial reuse of seawater concentrate using bipolar membrane electrodialysis. *Journal of Membrane Science*, 2014, 449: 119–126
41. Ghyselbrecht K, Silva A, Van der Bruggen B, Boussu K, Meesschaert B, Pinoy L. Desalination feasibility study of an industrial NaCl stream by bipolar membrane electrodialysis. *Journal of Environmental Management*, 2014, 140: 69–75
42. Davis J, Chen Y, Baygents J, Farrell J. Production of acids and bases for ion exchange regeneration from dilute salt solutions using bipolar membrane electrodialysis. *ACS Sustainable Chemistry & Engineering*, 2015, 3(9): 2337–2342